Multi-Polarization Superposition Beamforming with XPD-Aware Transmit Power Allocation

Paul Oh and Sean Kwon†
Department of Electrical Engineering, California State University, Long Beach
Email: Paul.Oh@student.csulb.edu
†Sean.Kwon@csulb.edu

2020 IEEE 92nd Vehicular Technology Conference (VTC2020-Fall) | 978-1-7281-9484-4/20/$31.00 ©2020 IEEE | DOI: 10.1109/VTC2020-Fall49728.2020.9348706

***Abstract*—The 5th generation (5G) new radio (NR) access technology and the future wireless communication require extremely high data rate and spectrum efficiency. Energy-efficient transmission/reception schemes are also regarded as an important component in 5G and beyond-5G communication systems. Based on this motivation, the polarization domain has attracted substantial attention; however, is not as fully utilized in a systematic manner as conventional time, frequency, and spatial domains. This paper is the first to propose *multi-polarization superposition beamforming (MPS-Beamforming)* with cross-polarization discrimination (XPD)-aware transmit power allocation utilizing the 5G antenna panel structure. The detailed mathematical derivation along with comprehensive simulation results are provided. Both the theoretical analysis and simulation results exhibit that the proposed scheme of MPS-Beamforming is significantly beneficial to the improvement of the performance in terms of the symbol error rate (SER) and signal-to-noise ratio (SNR) at the user equipment (UE). For instance, one of the simulation results in a practical scenario exhibits 7.5 dB SNR gain for 7×10^{-3} SER.**

I. Introduction

The 5th generation (5G) wireless communication system is to be first commercialized in 2020, and it is expected to be stabilized during several following years. 5G new radio (NR) access technology is a furnace of almost all the renowned communication theories and technologies. One of the key features that 5G NR supports is the full utilization of multiple-input multiple-output (MIMO) beamforming, so called, hybrid beamforming. Multiple antenna panels will be supported by the base station (BS) or equivalently, the next-generation Node B (gNB) following the agreement on the new name of the BS in 5G NR as illustrated in Fig. 1. Each antenna panel has multiple collocated dual-polarization antenna elements, where 8-by-8 dual-polarization antenna array has been regarded as one of the strongest candidates in 5G NR.

On the other hand, future wireless communication systems, including advanced revision of 5G similar to Long Term Evolution (LTE)-Advanced in 4G, will demand energy efficiency for, so called, green communications along with far higher channel capacity and spectrum efficiency than 5G. Consequently, this is the time for leading researchers and scholars to consider novel energy-efficient wireless communication schemes in addition to the current state-of-the-art in 5G NR. Based on the agreements achieved so far by the 5G standard society, 5G beamforming is supported by antenna subarray that consists of several spatially separated antenna elements in one column of the antenna panel with the same polarization, whether it is $+45^{\text{o}}$ or -45^{o} polarization. Although the gNB in 5G NR will support dual-beamforming with both $+45^{\text{o}}$ and -45^{o} polarization generated by the aforementioned antenna subarray, the current 5G NR design does not consider the impact of dual-beamforming on the polarization of the superimposed received signal at the end of user equipment (UE), which was previously or conventionally called mobile station (MS). Based on this motivation, this paper provides novel schemes along with the comprehensive analysis and simulation results for the impact of multi-polarization superposition beamforming (MPS-Beamforming) on the symbol error rate (SER) and the energy efficiency in terms of the signal-to-noise ratio (SNR) to meet a SER at the UE based on the orthogonal frequency division multiplexing (OFDM) system.

The polarization domain has been attracting substantial attention, and interesting research is being vigorously fulfilled in several aspects of utilizing polarization domain in these days. It includes, but is not limited to the recent achievements [1]–[14]. Utilizing the polarization domain has significant potential to achieve the aforementioned mission for the future wireless communication system, since even 5G NR is not fully utilizing the polarization domain in a systematic manner, e.g., based on full channel state information (CSI) of polarization. Utilizing polarization domain has shown large potential to increase channel capacity and spectral efficiency; and to reduce reduce bit/symbol error rate (BER/SER) [12], [15]–[19]. For this reason, impact of polarization on the performance of the wireless communication systems has been attracted substantial attention [12], [20]–[24]. It has been reported that the improvement of system performance via using multi-polarization antenna elements significantly depends on the condition of wireless channels [15]–[17]. The reason is that different conditions of wireless channels cause different degrees of channel depolarization. That is, the electromagnetic plane waves transmitted with a fixed polarization, e.g., -45^{o} polarization at the the gNB have both the copolarization (-45^{o}) and the cross-polarization ($+45^{\text{o}}$) components at the end of the UE. This symptom is called depolarization, and reported by the empirical and theoretical research [22]–[25]. The polarization misalignment between the transmitter (Tx) and the receiver (Rx) degrades the system performance in several aspects including the received signal power.

It is no doubt that the polarization domain has its unique

978-1-7281-9484-4/20/$31.00 ©2020 IEEE

characteristics distinct from the spatial domain in MIMO [12], [22], [24], [26]. The wireless communication system with multi-polarization needs to fully utilize the unique characteristics of polarized channels, in the same fashion that conventional MIMO system exploits spatial diversity of wireless channels. Furthermore, combining the utilization of polarization and spatial diversity in MIMO communication system can provide the improvement of the system performance in terms of channel capacity and BER [12], [15]–[17]. In particular, the improvement of channel capacity in the MIMO system with polarization-agile antennas is precisely described in [12]. Comprehensive understanding of polarization/depolarization in wireless communication systems from the measurement and modeling to the theory and novel schemes have been provided in aforementioned prior works.

Compared with the aforementioned prior literature, this paper has unique contributions. Appreciable contributions of this paper are summarized as follows:

- providing novel scheme of energy-efficient MPS-Beamforming based on cross-polarization discrimination (XPD)-aware transmit power allocation aligned with 5G antenna structure;
- theoretical analysis for the impact of combining transmit beams with different polarization and transmit power ratio on the polarization and power of the received signal, and SER;
- comprehensive simulation results and analysis illustrating the performance of the OFDM based MPS-Beamforming in terms of SER; and the relation of XPD with angle of rotation of the polarization ellipse for the received signal.

The remainder of this paper is as follows. Section II presents the system model for the energy-efficient MPS-Beamforming to be applied to. The system model is aligned with the 5G NR design agreed so far by the international standard society. Mathematical derivation and the corresponding theoretical interpretation are provided in Section III. Further, in Section IV, comprehensive analyses of the proposed scheme is provided via simulations. Finally, Section V concludes the paper.

II. System Model

We take into account the 5G NR system, where the gNB deploys multiple antenna panels to support Tx beamforming as described in Fig. 1. Based on the current agreements of the international standard society, each antenna panel has multiple antenna elements; each cross represents collocated dual-polarization antenna elements with fixed polarization, $\pm 45^o$. Notice that 8×8 antenna array with dual-polarization in the antenna panel has been regarded as one of the strongest candidates in 5G NR to be commercialized in 2020. An antenna subarray consists of one column or half column of the antenna panel.

The gNB in Fig. 1 utilizes uniform linear phase antenna subarrays, i.e., antenna elements in a column with one polarization among $\pm 45^o$. Further, the gNB can transmit a single data stream utilizing dual Tx beams, which have $+45^o$ and -45^o polarization at the side of the gNB. On the other hand, the receive antenna polarization at the UE can be changed owing to the movement of the user. Without the loss of generality, the polarization vector of the received signal supported by -45^o polarization beamforming at the gNB is set to be aligned with a vector $\overline{a_x}$; and $\overline{a_y}$ is for the received signal's polarization caused by $+45^o$ polarization beamforming at the gNB. The polarization of the received signals generated by $\pm 45^o$ polarization beamforming can be regarded as orthogonal in particular, for the LoS path. For the NLoS path, it can be also orthogonal in case of 5G beamforming from the channel modeling perspective in [24], as far as the beam is efficiently narrow, and single-bounced waves are the only component.

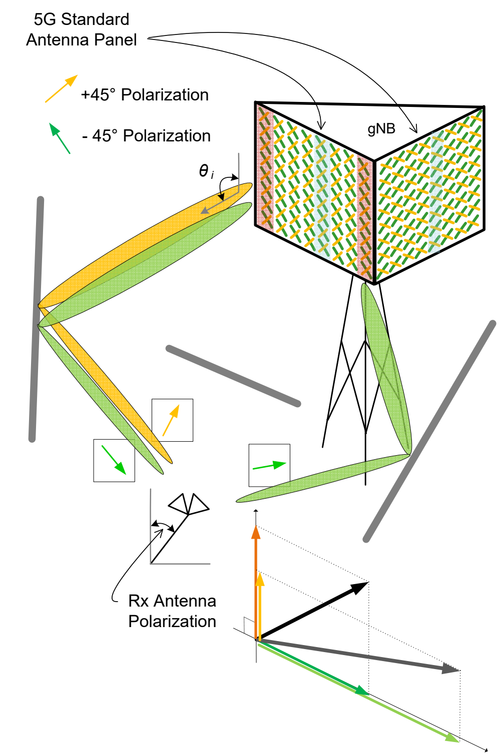

Fig. 1. 5G beamforming supported by multiple antenna panels at the gNB side agreed by the standard society.

The received signals at the UE, supported by -45^o and $+45^o$ polarization Tx beamforming, $r^{-45}(t,\tau_1)$ and $r^{+45}(t,\tau_2)$, respectively, can be expressed as following [27].

$$\begin{aligned} r^{-45^o}(t,\tau_1) &= \overline{a_x}\ E_x(t,\tau_1)\ A(\theta_1) \\ &= \overline{a_x}\ E_x A(\theta_1)\ \cos(2\pi f_c(t-\tau_1)+\phi_1) \\ &= \overline{a_x}\ E^{-45^o}\ \cos(2\pi f_c(t-\tau_1)+\phi_1), \end{aligned} \tag{1}$$

$$\begin{aligned} r^{+45^o}(t,\tau_2) &= \overline{a_y}\ E_y(t,\tau_2)\ A(\theta_2) \\ &= \overline{a_y}\ E_y A(\theta_2)\ \cos(2\pi f_c(t-\tau_2)+\phi_2) \\ &= \overline{a_y}\ E^{+45^o}\ \cos(2\pi f_c(t-\tau_2)+\phi_2), \end{aligned} \tag{2}$$

where for $i \in \{1,2\}$,

$$A(\theta_i) = \frac{\sin(N\psi_i/2)}{\sin(\psi_i/2)}, \tag{3}$$

$$\psi_i = \frac{2\pi}{\lambda} d\cos\theta_i + \zeta_i\ . \tag{4}$$

In (1) – (4), τ_i, ϕ_i, and θ_i for $i \in \{1, 2\}$ are the path delay, random phase component, and the angle between the line of the linear phase array and the direction of radio propagation, respectively. Further, ζ_i is the phase shift between progressive elements in the phase antenna array, and $A(\theta_i)$ is called antenna array pattern or array factor [27]. Lastly, λ and d are the wavelength and the distance between the consecutive elements in the phase antenna array.

While we focus on the expression of polarization for radio propagation in Mathematical representation in (1) – (4), the representation of the baseband signals are also utilized for both theoretical analysis and simulation in this paper. Aligned with 4G LTE and 5G NR standard, the OFDM system is the fundamental scenario in this paper; after RF demodulation and discrete Fourier transformation (DFT) at the Rx, the received signals on the n-th OFDM subcarrier at the antennas of the Rx with -45° and 45° polarization, $Y_n^{-45^{\circ}}$ and $Y_n^{45^{\circ}}$, respectively, can be obtained. In the case that no cross-polarized signal exists, $Y_n^{-45^{\circ}}$ and $Y_n^{45^{\circ}}$, are respectively,

$$Y_n^{-45^{\circ}} = \sqrt{E_s} H_n^{(-45^{\circ},-45^{\circ})} s(n) + w_n^{-45^{\circ}} \ , \tag{5}$$

$$Y_n^{45^{\circ}} = \sqrt{E_s} H_n^{(45^{\circ},45^{\circ})} s(n) + w_n^{45^{\circ}} \ , \tag{6}$$

where E_s is the energy of the transmitted information symbol, and n is the OFDM subcarrier index. $w_n^{-45^{\circ}}$ and $w_n^{45^{\circ}}$ are, respectively, the noise at the Rx antennas with -45° and 45° polarization. Finally, $H_n^{(-45^{\circ},-45^{\circ})}$ and $H_n^{(45^{\circ},45^{\circ})}$ are frequency-domain channel coefficients between the Tx and Rx antennas with -45° and 45° polarization, respectively. The cross-polarized received signal components will be taken into account in detail in Section III.

III. Energy-Efficient Multi-Polarization Superposition Beamforming (MPS-Beamforming)

The system model described in Fig. 1 and the associated theoretical representation in Section II imply that the polarization of the superimposed beams at the Rx of the UE must be affected by the transmit power and the phase shift in the array factors in (1) – (4). That is, the polarization for the superposition of transmit beams is primarily dependent on $E^{-45^{o}} = E_x A(\theta_1)$ and $E^{+45^{o}} = E_y A(\theta_2)$ in (1) – (4). Further, consideration of the cross-polarized received signals can make it feasible that transmit power allocation between -45° and 45° Tx beam can adjust the polarization of the received signals.

A. Novel Scheme of XPD-Aware Transmit Power Allocation for MPS-Beamforming

The OFDM system is the fundamental scenario in both the theoretical analysis and simulation in this paper to be aligned with the 4G LTE and 5G NR standards. Taking the impact of cross-polarized received signals at the Rx into account, the received signals on the n-th OFDM subchannel at the antennas of the Rx with -45° and 45° polarization, $Y_n^{-45^{\circ}}$ and $Y_n^{45^{\circ}}$, respectively, can be express as follows.

$$\begin{aligned} Y_n^{-45^{\circ}} &= \sqrt{\alpha E_s} H_n^{(-45^{\circ},-45^{\circ})} s(n) \\ &\quad + \sqrt{\beta E_s} H_n^{(-45^{\circ},45^{\circ})} s(n) + w_n^{-45^{\circ}} \ , \end{aligned} \tag{7}$$

$$\begin{aligned} Y_n^{45^{\circ}} &= \sqrt{\alpha E_s} H_n^{(45^{\circ},-45^{\circ})} s(n) \\ &\quad + \sqrt{\beta E_s} H_n^{(45^{\circ},45^{\circ})} s(n) + w_n^{45^{\circ}} \ , \end{aligned} \tag{8}$$

where the transmit power allocation ratio, α and β has the relation of $\beta = 1-\alpha$, and in the scenario without the proposed MPS-beamforming, $\alpha = 1$ or 0. In the scenario of MPS-Beamforming, $0 \le \alpha \le 1$; consequently, $0 \le \beta = 1 - \alpha \le 1$.

The statistical Rx cross-polarization discrimination (XPD) over all the subcarriers for the Tx antennas with -45° and 45° is defined with the double signs in same order as

$$\overline{\mathrm{XPD}}^{(\pm 45^{\circ})} \triangleq \frac{\sum_{n=1}^{N} \left| H_n^{(-45^{\circ},\pm 45^{\circ})} \right|^2}{\sum_{n=1}^{N} \left| H_n^{(45^{\circ},\pm 45^{\circ})} \right|^2}, \tag{9}$$

where once again, n is the subchannel index. Based on (7) – (8), the XPD of the received signal in the scenario of MPS-beamforming can be estimated is as following.

$$\begin{aligned} \overline{\mathrm{XPD}}^{\mathrm{MPS}} &\triangleq \frac{\mathrm{E}\big[|\sqrt{\alpha E_s} H_n^{(-45^{\circ},-45^{\circ})} + \sqrt{\beta E_s} H_n^{(-45^{\circ},45^{\circ})}|^2\big]}{\mathrm{E}\big[|\sqrt{\alpha E_s} H_n^{(45^{\circ},-45^{\circ})} + \sqrt{\beta E_s} H_n^{(45^{\circ},45^{\circ})}|^2\big]} \\ &= \frac{\alpha + \beta / \overline{\mathrm{XPR}}^{(-45^{\circ})}}{\alpha / \ \overline{\mathrm{XPD}}^{(-45^{\circ})} \ + \beta / \big(\ \overline{\mathrm{XPD}}^{(45^{\circ})} \overline{\mathrm{XPR}}^{(-45^{\circ})} \big)} \end{aligned} \tag{10}$$

where once again, n is the subcarrier index; and the received signal power ratio at the Rx antenna with -45° from Tx antennas with -45° and 45° polarization is called Rx cross-polarization ratio (XPR). In the similar manner with the statistical Rx XPD, the statistical Rx XPR is defined as

$$\overline{\mathrm{XPR}}^{-45^{\circ}} \triangleq \frac{\mathrm{E}[|H_n^{(-45^{\circ},-45^{\circ})}|^2]}{\mathrm{E}[|H_n^{(-45^{\circ}, \ 45^{\circ})}|^2]} \ . \tag{11}$$

Finally, the Tx allocates the transmission power to the Tx antennas with -45° and 45° polarization in the conventional scenario of the fixed total transmission power constraint. In other words, the Tx determines transmit power allocation ratio, α and consequently, $\beta = 1 - \alpha$; and the objective is to align $\overline{\mathrm{XPD}}^{\mathrm{MPS}}$ with the Rx antenna polarization, $\overline{\mathrm{XPD}}^{\mathrm{Rx-Ant}}$, i.e.,

$$\overline{\mathrm{XPD}}^{\mathrm{MPS}} = \overline{\mathrm{XPD}}^{\mathrm{Rx-Ant}} \ . \tag{12}$$

It is worth of notice that $\overline{\mathrm{XPD}}^{\mathrm{Rx-Ant}}$ can be changed by the rotation of antenna origination at the UE, caused by the movement of the UE.

B. Rotation Angle of the Polarization Ellipse in MPS-Beamforming

The mathematical derivation in this section describes that the polarization of MPS-Beamforming can be the elliptical polarization as portrayed in Fig. 2 even for the line-of-sight

(LoS) scenario. It is noteworthy that the LoS scenario is practical and essential one in 5G beamforming.

At the side of the UE, the superposition of the two signals, $r^{-45^o}(t,\tau_1)$ and $r^{+45^o}(t,\tau_2)$, impinges on the Rx antenna. That is,

$$\begin{aligned} r(t,\tau_1,\tau_2) &= r^{-45^o}(t,\tau_1) + r^{+45^o}(t,\tau_2) \\ &= \overline{a_x} E^{-45^o}\cos(\varphi) + \overline{a_y} E^{+45^o}\cos(\varphi+\Delta), \end{aligned} \tag{13}$$

where

$$\varphi = 2\pi f_c(t-\tau_1) + \phi_1 \ , \tag{14}$$

$$\Delta = -2\pi f_c(\tau_2-\tau_1) + (\phi_2-\phi_1) \ . \tag{15}$$

It is worth mentioning that Δ is the phase difference between (1) and (2), and in the scenario of line-of-sight (LoS) beamforming, $\Delta = 0$. Notice that it is prevalent view that LoS beamforming will be a dominant component; on the other hand, in the scenario of non line-of-sight (NLoS) beamforming, single-bounced beamforming may be feasible, even though some groups in international standard society and academia disagree with the bounced beamforming.

It is noteworthy that gNB can rotate the polarization ellipse, i.e., the major and minor axes of the polarization ellipse at the UE side via utilizing the proposed scheme, MPS-Beamforming. Furthermore, MPS-Beamforming can also change the eccentricity of the polarization ellipse; as the polarization ellipse becomes narrow and long, i.e., eccentricity comes to be very high, more received signal power can be concentrated on the direction of polarization ellipse's major axis.

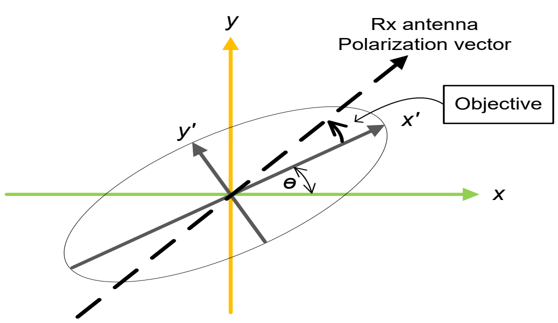

Fig. 2. Polarization ellipse and the rotation of the ellipse.

Based on the trigonometric identity for (1) – (2), the polarization of the superimposed signal at the UE, $r(t,\tau_1,\tau_2)$ in (13) can be derived as

$$\frac{E_y(t,\tau_2)}{E^{+45^o}} = \cos\varphi\cos\Delta - \sin\varphi\sin\Delta, \tag{16}$$

$$\frac{E_x(t,\tau_1)}{E^{-45^o}} = \cos\varphi, \tag{17}$$

$$\Rightarrow \ \frac{E_y(t,\tau_2)}{E^{+45^o}} = \frac{E_x(t,\tau_1)}{E^{-45^o}}\cos\Delta - \sin\varphi\sin\Delta \tag{18}$$

$$\begin{aligned} \Rightarrow \ &\left(\frac{E_x(t,\tau_1)}{E^{-45^o}\sin\Delta}\right)^2 + \left(\frac{E_y(t,\tau_2)}{E^{+45^o}\sin\Delta}\right)^2 \\ &\qquad - 2\frac{E_x(t,\tau_1)E_y(t,\tau_2)}{E^{-45^o}E^{+45^o}}\frac{\cos\Delta}{\sin^2\Delta} = 1. \end{aligned} \tag{19}$$

Finally, rotating the coordinates verifies that the polarization of the superimposed signal at the UE is elliptic as followings.

$$\left(\frac{E'_x(t,\tau_1)}{a}\right)^2 + \left(\frac{E'_y(t,\tau_2)}{b}\right)^2 = 1, \tag{20}$$

where

$$\begin{bmatrix} E'_x(t,\tau_1) \\ E'_y(t,\tau_2) \end{bmatrix} = \begin{bmatrix} \cos\theta & \sin\theta \\ -\sin\theta & \cos\theta \end{bmatrix} \begin{bmatrix} E_x(t,\tau_1) \\ E_y(t,\tau_2) \end{bmatrix}. \tag{21}$$

Comparing (19) and (20) after plugging in (21) – (21) into (20), the angle of rotation θ is described as

$$\begin{aligned} \theta &= \frac{1}{2}\tan^{-1}\left(\frac{2\cos\Delta}{\frac{E^{-45^o}}{E^{+45^o}} - \frac{E^{+45^o}}{E^{-45^o}}}\right) \\ &= \frac{1}{2}\tan^{-1}\left(\frac{2\cos\Delta}{\sqrt{\mathrm{XPD}} - 1/\sqrt{\mathrm{XPD}}}\right). \end{aligned} \tag{22}$$

It is worth emphasizing that the rotation angle of the polarization ellipse, θ, is the functions of E^{-45^o}/E^{+45^o}, where instantaneous Rx XPD can be defined as $(E^{-45^o}/E^{+45^o})^2$ following the convention in the research area of the polarization in wireless communications. The XPD is usually defined as the power ratio of two orthogonal polarization components, in this section, E^{-45^o} and E^{+45^o} components.

IV. Simulation Results

This section provides comprehensive simulation results and the associated analysis for MPS-Beamforming with XPD-aware transmit power allocation. The SER performance of the MPS-Beamforming in the OFDM system with the fundamental modulation of quadrature phase shift keying (QPSK) shows 7.5 dB SNR gain in a realistic scenario. It is shown that the instantaneous Rx XPD affects the rotation angle of the Rx polarization ellipse at the UE. A variety of phase difference, Δ in (13) – (15) along with varying $\mathrm{XPD} = (E^{-45^o}/E^{+45^o})^2$ are taken into account. Further, several Rx antenna polarization angles at the UE are considered to reflect the movement of the UE on the rotation of the Rx antenna orientation. Although some prior research defines XPD in slightly different manners, we follow the prevalent conventional definition of instantaneous or statistical XPD, which is described in Section III.

The polarization angle of the superimposed received signal at the UE, θ, is a function of XPD as demonstrated in (22). The behavior of θ is depicted for varying XPD and a variety of phase difference in Fig. 3. When XPD is unity in linear scale, it yields $\theta = 45^o$ for all the scenarios with respect to the phase difference. In the coordinates described in Figs. 1 and 2, E^{-45^o} is the component for x-axis; therefore, as XPD increases, the polarization on x-axis increases, corresponding to the scenario that θ converges to zero.

Fig. 4 represents the received signal power when Rx antenna polarization is 0^o. In the scenario that $\Delta = 0^o$, and $\mathrm{XPD} = 1$; $\theta = 45^o$. That is, the polarization of the received signal is exactly aligned with the Rx antenna polarization; thus, the received signal power will be maximized. As illustrated in

Fig. 4, comparing to the scenario of no MPS-Beamforming, i.e., $E^{+45^o} = 0$ or equivalently, XPD = ∞, MPS-Beamforming with XPD = 1 can save 35% of transmission power in coherent MPS-Beamforming ($\Delta = 0^o$). Nonetheless, when $\Delta < 45^o$, the UE can still expect approximately 85% of the maximum received signal power.

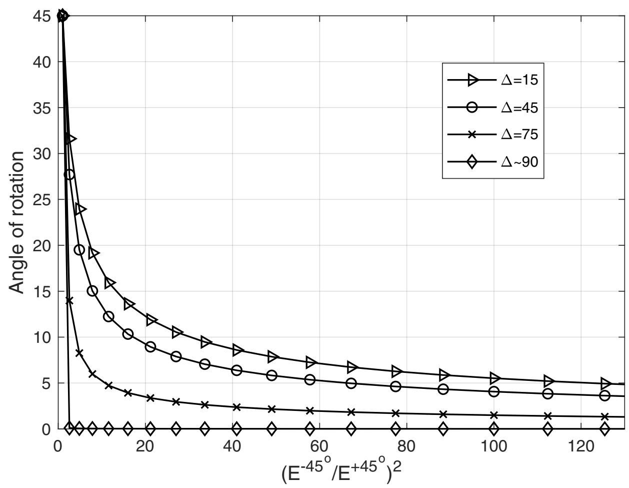

Fig. 3. Angle of Rotation, θ vs. XPD.

They are impressive results describing that the proposed MPS-Beamforming is significantly energy efficient, i.e., we can minimize power loss when the polarization ellipse is well aligned to the Rx antenna polarization.

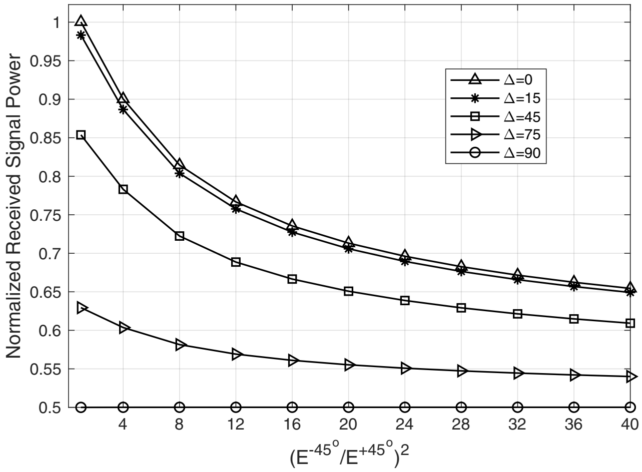

Fig. 4. Received signal power when Rx antenna polarization is 0^o

The SER performance of the OFDM system with MPS-Beamforming and XPD-aware transmit power allocation is illustrated in Figs. 5–7. They are the simulation results for the same channel with 12 dB $\overline{\mathrm{XPD}}^{(-45^o)}$, but with different Rx antenna polarization, $\overline{\mathrm{XPD}}^{\mathrm{Rx-Ant}}$. In other words, the statistical XPD for the transmit beamforming with -45^o polarization, $\overline{\mathrm{XPD}}^{(-45^o)} = 2^4$ in linear scale. Following the 5G NR standard, the Rx antenna polarization angle varies between -45^o and 45^o; and $\tan(45^o - \mathrm{Rx\ antenna\ polarization\ angle}) = \overline{\mathrm{XPD}}^{\mathrm{Rx-Ant}}$ in linear scale. The simulation results apparently show that MPS-Beamforming with the XPD-aware transmit power allocation significantly improves the OFDM based system performance in terms of SER. For instance, in the scenario of Fig. 7, the MPS-Beamforming with XPD-aware transmit power allocation ratio, $\alpha = 0.5$ has 7.5 dB gain of the SNR for 7×10^{-3} SER comparing with the case of no MPS-Beamforming, i.e., $\alpha = 0$. The different Rx antenna polarization requires different transmit power allocation ratios as illustrated in the legend associated with the lowest curve at each figure.

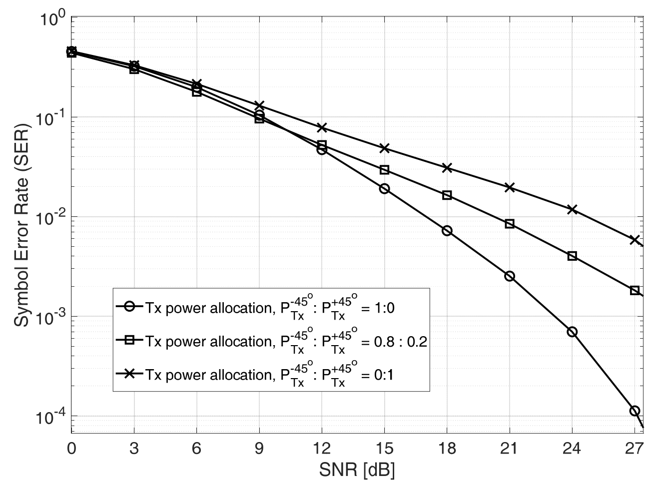

Fig. 5. Symbol error rate for different transmit power allocation in the scenario of Rx antenna polarization of -45^o with 12 dB $\overline{\mathrm{XPD}}^{(-45^o)}$

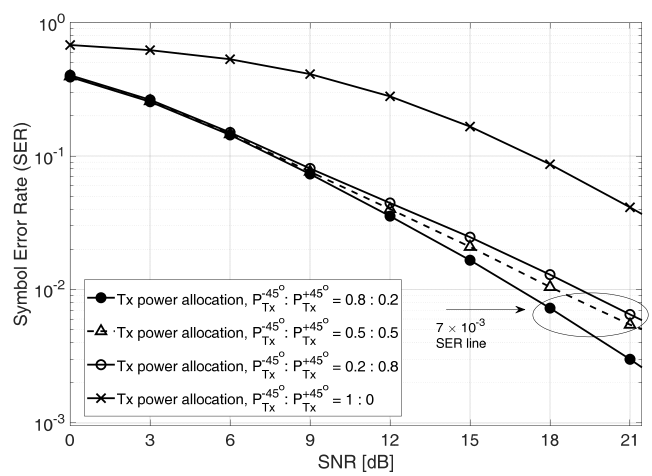

Fig. 6. Symbol error rate for different transmit power allocation in the scenario of Rx antenna polarization of -30^o with 12 dB $\overline{\mathrm{XPD}}^{(-45^o)}$

The Rx antenna polarization is varying among the three different values, -45^o, -30^o and 0^o in Figs. 5, 6 and 7, respectively. The corresponding values of α are $\alpha = 1$, $\alpha = 0.8$ and $\alpha = 0.5$; it is noteworthy that $\alpha = 1$ is the case of single transmit beam with -45^o polarization. In the scenario

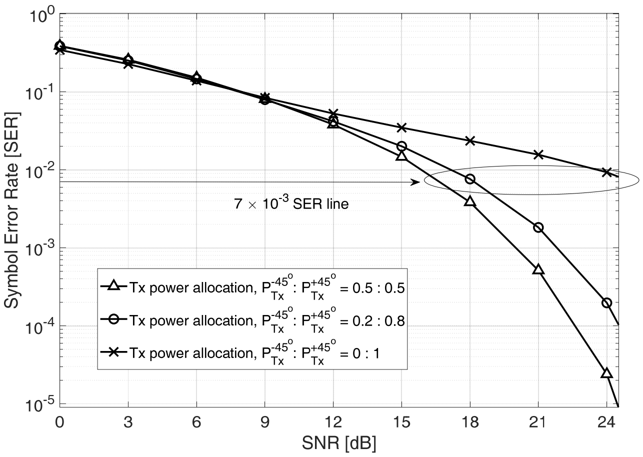

Fig. 7. Symbol error rate for different transmit power allocation in the scenario of Rx antenna polarization of 0^o with 12 dB $\overline{\mathrm{XPD}}^{(-45^o)}$

of -30^o or 0^o Rx antenna polarization in Fig. 6 or 7, the value of α which satisfies (12) with (10) – (10), are $\alpha = 0.8$ or $\alpha = 0.5$, respectively as described in the legend of Fig. 6 or 7. In each scenario of Rx antenna polarization, the proposed XPD-aware transmit power allocation with the theoretically obtained α based on (12) with (10) – (10), outperforms that of any other choice of α.

V. Conclusion

This paper is the first to propose a novel scheme of MPS-Beamforming along with XPD-aware transmit power allocation. Based on the 5G antenna panel structure agreed by the 5G NR standard society, the proposed scheme can be utilized to have the significant benefit of improving SER and thus, energy efficiency. The comprehensive simulation results show remarkable improvement including 7.5 dB SNR gain for 7×10^{-3} SER in a realistic scenario. The scheme of MPS-Beamforming has the significant potential to be utilized in the advanced revision of 5G NR and beyond-5G wireless communication standard and systems in the future.

References

[1] S. H. Doan, S. Kwon, and H. Yeh, "Achievable capacity of multipolarization MIMO with the practical polarization-agile antennas," *IEEE Systems Journal*, Jun. 2020.

[2] J. Zhang, K. J. Kim, A. A. Glazunov, Y. Wang, L. Ding, and J. Zhang, "Generalized polarization-space modulation," *IEEE Trans. Commun.*, vol. 68, no. 1, pp. 258–273, Jan. 2020.

[3] K. Satyanarayana, T. Ivanescu, M. El-Hajjar, P. . Kuo, A. Mourad, and L. Hanzo, "Hybrid beamforming design for dual-polarised millimetre wave MIMO systems," *IET Electronics Let.*, vol. 54, no. 22, pp. 1257–1258, 2018.

[4] X. Zhang, B. Zhang, and D. Guo, "Performance of poly-polarization multiplexing in narrow-band wireless communication aided by pre-compensation and multi-notch OPPFs," *IEEE Wireless Commun. Let.*, vol. 6, no. 4, pp. 478–481, Aug 2017.

[5] G. Zafari, M. Koca, and H. Sari, "Dual-polarized spatial modulation over correlated fading channels," *IEEE Trans. Commun.*, vol. 65, no. 3, pp. 1336–1352, Mar. 2017.

[6] P.-Y. Qin, S.-L. Chen, and Y. J. Guo, "A compound reconfigurable microstrip antenna with agile polarizations and steerable beams," in *Antennas and Propagation (ISAP), 2017 International Symposium on*. IEEE, 2017, pp. 1–2.

[7] G. Wolosinski, V. Fusco, and O. Malyuskin, "2-bit polarisation agile antenna with high port decoupling," *Electronics Letters*, vol. 52, no. 4, pp. 255–256, 2016.

[8] S.-L. Chen, P.-Y. Qin, C. Ding, and Y. J. Guo, "Cavity-backed proximity-coupled reconfigurable microstrip antenna with agile polarizations and steerable beams," *IEEE Transactions on Antennas and Propagation*, vol. 65, no. 10, pp. 5553–5558, 2017.

[9] B. Babakhani, S. K. Sharma, and N. R. Labadie, "A frequency agile microstrip patch phased array antenna with polarization reconfiguration," *IEEE Transactions on Antennas and Propagation*, vol. 64, no. 10, pp. 4316–4327, 2016.

[10] H. Sun and S. Sun, "A novel reconfigurable feeding network for quad-polarization-agile antenna design," *IEEE Transactions on Antennas and Propagation*, vol. 64, no. 1, pp. 311–316, 2016.

[11] L.-P. Cai and K.-K. M. Cheng, "Continuously tunable polarization agile antenna design using a novel varactor-only signal control device," *IEEE Antennas and Wireless Propagation Letters*, vol. 16, pp. 1147–1150, 2017.

[12] S.-C. Kwon and A. F. Molisch, "Capacity maximization with polarization-agile antennas in the MIMO communication system," *Proc. IEEE Global Telecommun. Conf.*, pp. 1–6, Dec. 2015.

[13] Y.-J. Liao, H.-L. Lin *et al.*, "Polarization reconfigurable eccentric annular ring slot antenna design," *IEEE Transactions on Antennas and Propagation*, vol. 63, no. 9, pp. 4152–4155, 2015.

[14] S.-C. Kwon, "Optimal power and polarization for the capacity of polarization division multiple access channels," in *Proc. IEEE Global Telecommun. Conf.*, Dec. 2014, pp. 1–5.

[15] J. Jootar, J.-F. Diouris, and J. Zeidler, "Performance of polarization diversity in correlated Nakagami-m fading channels," *IEEE Transactions on Vehicular Technology*, vol. 55, no. 1, pp. 128–136, 2006.

[16] Y. Deng, A. Burr, and G. White, "Performance of MIMO systems with combined polarization multiplexing and transmit diversity," in *Proc. IEEE Veh. Technol. Conf.*, vol. 2, May 2005, pp. 869–873.

[17] R. Nabar, H. Bolcskei, V. Erceg, D. Gesbert, and A. Paulraj, "Performance of multiantenna signaling techniques in the presence of polarization diversity," *IEEE Trans. Sig. Proc.*, vol. 50, no. 10, pp. 2553–2562, Oct. 2002.

[18] S.-C. Kwon and G. Stüber, "Polarization division multiple access on NLoS wide-band wireless fading channels," *IEEE Trans. Wireless Commun.*, vol. 13, no. 7, pp. 3726–3737, Jul. 2014.

[19] S.-C. Kwon, "Geometrical theory, modeling and applications of channel polarization," *Ph.D. Thesis, Georgia Institute of Technology*, pp. 1–128, 2014.

[20] M. R. Andrews, P. P. Mitra, and R. deCarvalho, "Tripling the capacity of wireless communications using electromagnetic polarization," *Nature*, vol. 409, pp. 316–318, Jan. 2001.

[21] V. Erceg, P. Soma, D. Baum, and S. Catreux, "Multiple-input multiple-output fixed wireless radio channel measurements and modeling using dual-polarized antennas at 2.5 GHz," *IEEE Trans. Wireless Commun.*, vol. 3, no. 6, pp. 2288 – 2298, Nov. 2004.

[22] M. Shafi, M. Zhang, A. Moustakas, P. Smith, A. Molisch, F. Tufvesson, and S. Simon, "Polarized MIMO channels in 3-D: Models, measurements, and mutual information," *IEEE J. Sel. Areas Commun.*, vol. 24, no. 3, pp. 514–527, Mar. 2006.

[23] M. Landmann, K. Sivasondhivat, J.-I. Takada, I. Ida, and R. Thoma, "Polarisation behaviour of discrete multipath and diffuse scattering in urban environments at 4.5 GHz," *EURASIP J. Wireless Commun. Netw.*, no. 1, p. 60, Jan. 2007 Article ID 57980.

[24] S.-C. Kwon and G. L. Stüber, "Geometrical theory of channel depolarization," *IEEE Trans. Veh. Technol.*, vol. 60, no. 8, pp. 3542–3556, Oct. 2011.

[25] V. Erceg, H. Sampath, and S. Catreux-Erceg, "Dual-polarization versus single-polarization MIMO channel measurement results and modeling," *IEEE Trans. Wireless Commun.*, vol. 5, no. 1, pp. 28–33, Jan. 2006.

[26] S.-C. Kwon, G. Stüber, A. López, and J. Papapolymerou, "Geometrically based statistical model for polarized body-area-network channels," *IEEE Trans. Veh. Technol.*, vol. 62, no. 8, pp. 3518–3530, Oct. 2013.

[27] T. A. Milligan, *Modern Antenna Design*. Chichester, UK: John Wiley & Sons, Inc, 2005.